

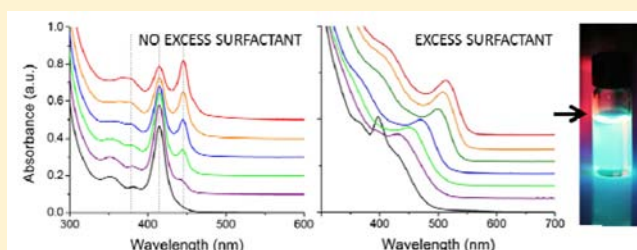
Surfactant-Controlled Polymerization of Semiconductor Clusters to Quantum Dots through Competing Step-Growth and Living Chain-Growth Mechanisms

Christopher M. Evans, Alyssa M. Love, and Emily A. Weiss*

Department of Chemistry, Northwestern University, Evanston, Illinois 60208-3113, United States

S Supporting Information

ABSTRACT: This article reports control of the competition between step-growth and living chain-growth polymerization mechanisms in the formation of cadmium chalcogenide colloidal quantum dots (QDs) from CdSe(S) clusters by varying the concentration of anionic surfactant in the synthetic reaction mixture. The growth of the particles proceeds by step-addition from initially nucleated clusters in the absence of excess phosphinic or carboxylic acids, which adsorb as their anionic conjugate bases, and proceeds indirectly by dissolution of clusters, and subsequent chain-addition of monomers to stable clusters (Ostwald ripening) in the presence of excess phosphinic or carboxylic acid. Fusion of clusters by step-growth polymerization is an explanation for the consistent observation of so-called “magic-sized” clusters in QD growth reactions. Living chain-addition (chain addition with no explicit termination step) produces QDs over a larger range of sizes with better size dispersity than step-addition. Tuning the molar ratio of surfactant to Se^{2-} (S^{2-}), the limiting ionic reagent, within the living chain-addition polymerization allows for stoichiometric control of QD radius without relying on reaction time.



INTRODUCTION

This paper describes the competition between two channels for the polymerization of cadmium chalcogenide clusters into colloidal quantum dots (QDs). We tune this competition by varying the concentration of either phosphinic or carboxylic acid in the synthetic reaction mixture; both of these acids adsorb to the clusters and QDs as their respective anionic conjugate bases, and serve as a ligand for Cd^{2+} . We therefore refer to these surfactants as “anionic ligands” in the remainder of this manuscript. With only a stoichiometric amount of ligand for the participating Cd^{2+} and Se^{2-} (or S^{2-}) ions present, fusion of clusters proceeds in discrete steps from the original nuclei, with kinetics and other properties characteristic of step-growth polymerization. When excess anionic ligand is present, some clusters first dissolve, and resulting monomers add to other clusters to produce a continuum of QD sizes over time, with kinetics and other properties characteristic of living chain-addition polymerization. The living chain-addition mechanism produces larger nanocrystals with a narrower size distribution than the step-addition mechanism. Within the chain-addition process, the final size of the particle is controllable through the stoichiometric ratio of anionic surfactant to Se^{2-} (or S^{2-}), the limiting ionic reagent.

Certain sizes of semiconductor clusters, the UV-absorbing precursors of colloidal quantum dots, have appeared with inordinate frequency during growth reactions since the earliest days of quantum dot (QD) synthesis.^{1–5} The reason for the consistent appearance of these sizes, as well as the mechanism of their formation and decay, has been controversial since their

first observation. Henglein and co-workers, in some of the earliest work on colloidal CdS, suggested that certain sizes of CdS were observed because they were integer multiples of a preferred base cluster.¹ This explanation, however, never gained widespread acceptance in the QD community and has since been replaced with the theory that some cluster sizes have geometries that give them exceptional thermodynamic stability; they were hence termed “magic-sized clusters”.^{2,6–9} Experimental evidence supporting the thermodynamic argument relies on matrix-assisted laser desorption/ionization time-of-flight mass spectrometry (MALDI-TOF MS) measurements that discovered persistent mass fragments in cluster samples.^{10,11} Fragments were assigned specific stoichiometries (e.g., $(\text{CdSe})_{13}$, $(\text{CdSe})_{19}$ and $(\text{CdSe})_{33}$) and geometries, based on close-packing arguments and first-principles calculations. The MALDI-TOF MS measurements, however, yielded the same mass distributions, whether analyzing bulk semiconductors or clusters, and produced the same fragmentation patterns for samples with different absorption spectra.¹⁰ These inconsistencies suggest that their results may not be representative of the actual distribution, but perhaps may be artifacts of the ionization process. Further, computational predictions for the thermodynamic preferences for magic clusters relative to their structural isomers and neighboring sizes are too small to account for the high degree of specificity for these sizes in most syntheses.^{11,12}

Received: August 10, 2012

Published: September 26, 2012

For much of the last three decades of QD synthesis, stable clusters existed merely as reaction byproducts; however, recent optimizations of QD synthesis, and the need for increased monodispersity of QD samples for optoelectronic¹³ and biological applications,^{14,15} renew the relevance of their mechanistic role in QD growth.^{16,17} We show here that the role of these clusters in QD growth depends on the amount of surfactant for the excess ion (here anionic surfactant for Cd^{2+}). As did Ozin and co-workers in a recent report on the growth of Bi_2S_3 nanowires,¹⁸ we identify two channels for growth of clusters into cadmium chalcogenide nanocrystals: a step-growth polymerization channel (the mechanism originally suggested by Henglein and co-workers¹) and a living chain-growth polymerization channel. In Ozin's system, these two channels contributed simultaneously; in our system, the step-growth mechanism is only operative in the absence of excess anionic surfactant. If excess surfactant is present, cluster dissolution provides monomer or smaller-cluster feedstock for a living chain-addition-like polymerization, which results in a larger range of sizes with better monodispersity than step-addition.

The step-growth process explains the repeated appearance of certain sizes of CdSe clusters from the original nuclei in the absence of excess surfactant. The dissolution step necessary for the chain-growth process to occur provides a means for controlling the size of the final QD product without relying on the time of reaction; the larger the excess of anionic surfactant in the reaction mixture, the faster the growth of the clusters and the smaller the final size of the QDs when the growth saturates due to lack of available monomer. Living chain-addition therefore provides a means for precise, reproducible synthesis of colloidal QDs.

RESULTS AND DISCUSSION

Clusters Polymerize by Step-Addition in the Absence of Excess Ligand. Figure 1a shows a series of absorption spectra, acquired over a period of ~ 17 min, of a reaction mixture of dicyclohexylphosphine selenide (DCHP Se) and Cd-diisooctylphosphinic acid (Cd-DIOP), where only stoichiometric amounts of the organophosphine and phosphinic acid are present, heated at 160°C in tetradecane. We chose these Cd and Se precursors because previous work demonstrated that their combination results in fast nucleation of CdSe clusters and immediate depletion of molecular reagents, even at room temperature, due to the high reactivity of secondary phosphine chalcogenide precursors.¹⁹ Rapid loss of monomeric precursors in a polymerization reaction is one characteristic of a step-growth mechanism, where fast-nucleated oligomers combine in a quantized way to form oligomers that are integer multiple units of the base unit. A step-growth of small clusters into larger clusters (see schematic in Figure 2) is, in fact, what we observe under these reaction conditions. Each observed absorbance peak that forms and disappears as the reaction proceeds is at a wavelength consistent with a cluster with a volume that is an integer multiple of the volume for the smallest cluster, $(\text{CdSe})_{n=1}$; these peaks are marked accordingly with vertical lines in Figure 1, and listed in Table 1. We estimate the $n = 1$ cluster, which absorbs at 332 nm, to be 0.91 nm in diameter, based on experimentally measured calibration curves of absorbance energy vs radius,²⁰ and to have the formula $(\text{CdSe})_7$, based on its volume. The clusters are too small to size accurately using transmission electron microscopy (TEM), however, and, as mentioned in the Introduction, it would be unclear whether the masses obtained from MALDI-TOF mass

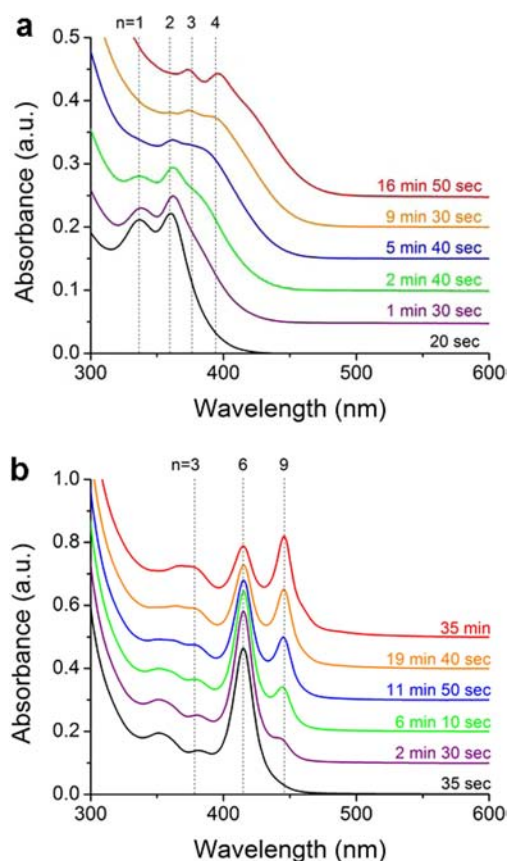


Figure 1. (a) Spectra for clusters heated with diisooctylphosphinic acid as the native ligand at 160°C in tetradecane. (b) Spectra for clusters heated with oleylamine as the native ligand at 200°C in oleylamine. The vertical lines show the positions of peaks (predicted from experimentally measured calibration curves of absorbance energy vs radius) for clusters that have integer multiples of the volume of the smallest cluster observed, marked $n = 1$ (see Table 1). The peaks between 350 and 375 nm represent higher-order transitions for the $n = 6$ and $n = 9$ clusters. Slight misalignment of the $n = 2$ peaks at different times (in a) and $n = 3$ peaks (in b) is due to convolution with other peaks in the spectrum. The Supporting Information (SI) contains an example of a deconvoluted spectrum that we used to assign peak energies. Over the range of wavelengths of the clusters we examined, small differences in cluster size result in detectable differences in wavelength—for instance, the absorption peaks for $(\text{CdSe})_3$ and $(\text{CdSe})_{3.25}$ (hypothetically) are separated by 4 nm.

spectroscopy are the original clusters or fragmentation products. The notation $((\text{CdSe})_{n=x})$ therefore only indicates the volume of the $n = x$ cluster relative to the volume of the $n = 1$ cluster.

If $(\text{CdSe})_{n=1}$, a sphere with a diameter of 0.91, doubled in volume, it would have a diameter of 1.15 nm and therefore absorb at 359 nm. This estimate coincides with the next highest energy peak observed at 360 nm; we call the $d = 1.15$ nm cluster $(\text{CdSe})_{n=2}$. Heating $(\text{CdSe})_{n=1}$ and $(\text{CdSe})_{n=2}$ together at 160°C produces new absorption peaks that closely match predictions for the absorbance of $(\text{CdSe})_{n=3}$ and $(\text{CdSe})_{n=4}$. Although we cannot directly measure the shape of these clusters with TEM, the fact that the volumes of the clusters predicted by calibration curves for spherical particles match closely with those of clusters observed in experimental absorption data supports the validity of the assumption of a quasi-spherical shape. Further, extensive heating of small

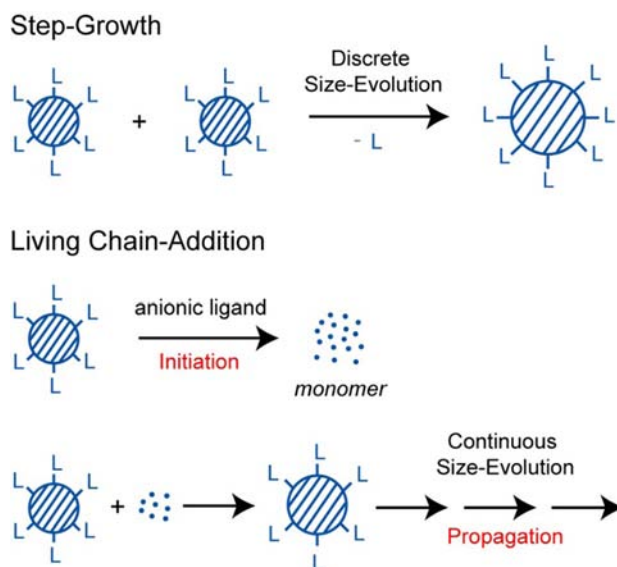


Figure 2. Schematic diagram of the step-growth and living chain-addition mechanisms responsible for nanoparticle growth. There is no explicit “termination” step in the chain-addition mechanism; termination occurs when the average size of the nanocrystals is large enough such that monomer feedstock is no longer produced by the initiation (dissolution) step.

clusters under step-growth conditions eventually produces nanocrystals of sufficient size for TEM imaging; in all cases they are spherical.

The step-growth mechanism we observe is not specific to the tetradecane system. When a mixture of $(\text{CdSe})_{n=1}$ and $(\text{CdSe})_{n=2}$ clusters (produced by the reaction described above) is exposed to neat oleylamine at room temperature, the clusters rapidly combine to form primarily $(\text{CdSe})_{n=6}$ (see the SI, Figure S1). After heating $(\text{CdSe})_{n=6}$ to 200 °C, a new absorption peak corresponding to the volume of a $(\text{CdSe})_{n=9}$ cluster appears, coincident with a decrease in the concentration of the $(\text{CdSe})_{n=6}$ species, Figure 1b. We can therefore conclude that the $n = 9$ cluster forms from the fusion of the $n = 6$ cluster with the smaller clusters, and not by independent nucleation.

Measurement of the integrated intensity of the 376-nm feature corresponding to $(\text{CdSe})_{n=3}$ in neat tetradecane as a function of time at 140, 160, 180, and 200 °C yields apparent zeroth-order rate constants for the rate-limiting process in the

disappearance of the clusters, and an activation barrier of 21.9 kcal mol⁻¹, Figure 3. $(\text{CdSe})_{n=3}$ is a convenient cluster to

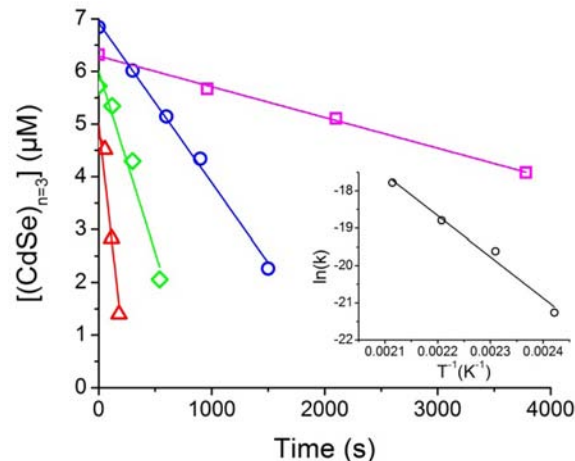


Figure 3. Concentration of $(\text{CdSe})_{n=3}$ clusters ($\lambda_{\text{abs}} = 376$ nm, calculated by integrating the absorbance peak for the cluster (see the SI) vs time at reaction temperatures of 140 (square), 160 (circle), 180 (diamond), and 200 (triangle) °C. The slopes of the lines are the zeroth-order rate constants for the rate-limiting process in the disappearance of the clusters; these slopes are (in order of increasing temperature) 5.8×10^{-10} , 3.0×10^{-9} , 6.9×10^{-9} and 1.9×10^{-8} M/s. (Inset) Plot of $\ln(k)$, where k is the rate constant for the disappearance of the clusters vs $1/T$ for disappearance of phosphinic acid-coated $(\text{CdSe})_{n=3}$ ($\lambda_{\text{abs}} = 376$ nm) clusters by cluster–cluster fusion. From the linear fit to the Arrhenius equation, we obtain the activation energy ($E_a = 21.9$ kcal/mol) for the rate-limiting step in the disappearance of clusters.

monitor because it reacts slowly enough to be observed across the chosen temperature range. Zeroth-order and pseudo-zeroth-order rate constants have also been observed previously for clusters coalescing into nanorods,¹⁶ and for the precipitation of thiol-capped CdTe²¹ and CdSe QDs.²² Both of these processes and the step-growth polymerization process we study here presumably proceed through approach of two ligand-passivated units, and subsequent desorption of ligands from the surfaces of the clusters to expose reactive surface ions. Removal of surface ligands must occur during the growth process since the total surface area of the particles decreases with fusion. We are currently investigating whether the compression of ligand

Table 1. Predicted Absorbance Wavelengths for the First Excitonic Transition of CdSe Clusters of Various Sizes and Experimentally Observed Absorbance Peaks from this Report and Others

$(\text{CdSe})_{n=}$	calcd abs. (nm) ^a	our work			ref 25	ref 6	ref 31	ref 26	ref 32
		R ₂ POOH	R'NH ₂						
1	332 ^b	332				330	332	336	331
2	359	361				360		363	355
3	376	374	379	380		383	380		376
4	391	395						389	
5	403					406	404	404	405
6	415		415	414				404	420
7	425						427	427	
8	436					431			
9	445		445	446		447			449

^aAbsorption wavelengths for clusters 2–9 were determined by adding an integer unit of volume to the base cluster (332 nm) and calculating the absorbance position from known sizing curves. ^bMeasured absorbance position from Figure 1.

shells upon collision of two units or desorption of ligands (probably via protonation of adsorbed ligands²³), or a combination, is rate-limiting and therefore responsible for the observed activation barrier for step-growth.

In addition to growth of nanocrystals in discrete steps, the reaction of clusters in the absence of excess ligand resembles step-growth polymerization in that (i) the concentration of our monomer unit (the cadmium and selenium precursors) decreases rapidly, concomitant with the appearance of the smallest observable cluster,¹⁹ and (ii) the polydispersity in size of the nanocrystal product increases with the degree of polymerization (see SI, Figure S5).²⁴

We found evidence for growth of CdSe QDs in discrete fusion steps in absorption spectra within several literature reports (Table 1). For example, the cluster species observed by Dukes, III. et al. can be rationalized as a direct consequence of fusion reactions between $(\text{CdSe})_{n=3}$ (386 nm), $(\text{CdSe})_{n=6}$ (414 nm), and $(\text{CdSe})_{n=9}$ (446 nm) species concurrently in solution.²⁵ Liu et al. observed absorbance peaks form consecutively at 425, 485, 518, and 548 nm at 118–122 °C; these peaks correspond to $(\text{CdSe})_{n=7}$, $(\text{CdSe})_{n=14}$, $(\text{CdSe})_{n=21}$, and $(\text{CdSe})_{n=35}$.²⁶ We suspect that not every combination of clusters appears because only clusters that exist in appreciable quantities simultaneously are capable of reacting. For example, $(\text{CdSe})_{n=7}$ and $(\text{CdSe})_{n=21}$ never coincide in appreciable quantities, so Liu does not observe a peak corresponding to $(\text{CdSe})_{n=28}$. There are also examples in the literature of the step-growth of CdS clusters; Table 2 presents two exam-

Table 2. Measured Absorbance Wavelengths for CdS Clusters from Literature Reports, and Corresponding Diameters and Volumes

$(\text{CdS})_n$ $n =$	absorption position (nm)	diameter (nm) ^a	normalized volume
Zanella et al. ^b			
2	303	1.41	1.0
3	326	1.66	1.6
6	347	2.01	2.9
9	363	2.35	4.6
15	378	2.73	7.3
Li et al. ^c			
3	322	1.61	1.5
6	349	2.05	3.1
9	361	2.31	4.4
15	379	2.76	7.5

^aDiameters determined from sizing curves. ^bReference 27. ^cReference 28.

ples.^{27,28} Both reports list cluster absorbances at similar positions. The second-smallest cluster observed (326 and 322 nm in the two reports) is only a factor of 1.5 larger than the smallest cluster absorbance recorded at 303 nm; thus, it is likely that the 303-nm cluster is not the smallest ($n = 1$) cluster produced in this reaction, but rather, it is the $n = 2$ cluster. Data from a report by Zanella et al. indicate that peaks corresponding to quantized diameters of QDs also appear during the growth of CdTe and ZnSe clusters.²⁷

A step-growth polymerization mechanism has also been implicated in the assembly of metal nanoparticles into higher-order structures,²⁹ growth of Bi_2S_3 nanowires,¹⁸ and growth of II–VI semiconductor and metal oxide nanorods (in the case of

anisotropic structures, the mechanism is usually called “oriented attachment”).^{6,25,26,30–34}

Quantum Dots Form by a Living Chain-Addition Polymerization in the Presence of Excess Anionic Ligand. In the previous section, we described a step-addition mechanism for growth of clusters. We only observe step-addition, however, when there is a stoichiometric amount of anionic surfactant in the reaction mixture. In the presence of excess anionic surfactant, the step-growth channel is out-competed by the dissolution of clusters, which then precipitates a chain-addition process. Figure 4 shows the absorption spectra

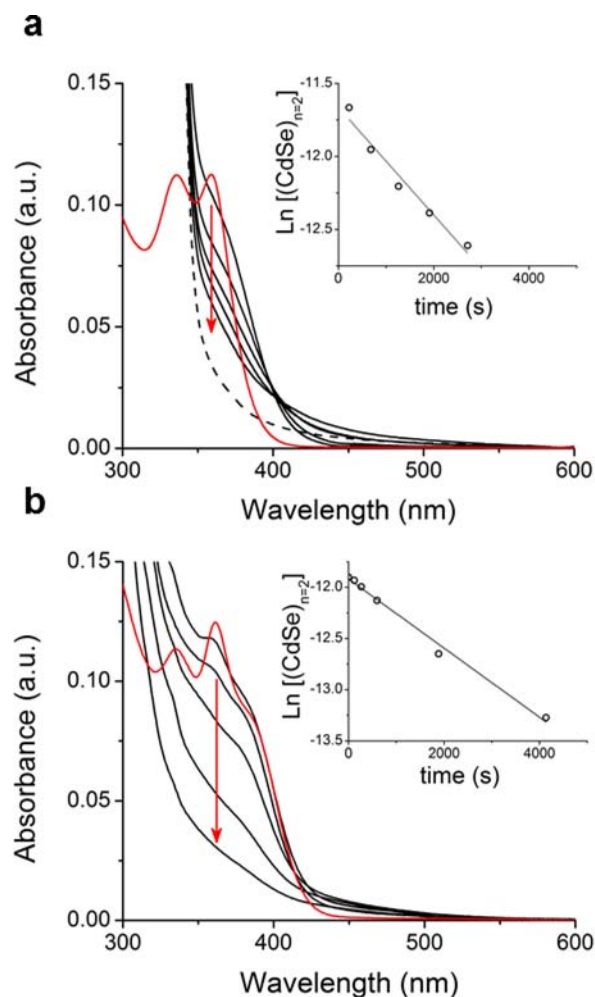


Figure 4. Optical absorption spectra for phosphinic acid-coated CdSe clusters heated to 60 °C in (a) oleic acid, and (b) diisooctylphosphinic acid. The clusters’ absorption spectra prior to heating are shown in red, while the times for each trace in panel a are (from top to bottom): 3 min 45 s, 11 min 21 s, 21 min 4 s, 31 min 51 s, and 45 min 10 s. The times for each trace in panel b are (from top to bottom): 50 s, 2 min, 10 min, 31 min 30 s, and 69 min. The observed decrease in optical density during heating is observed to follow a first-order kinetic decay (inset). The dotted line in panel a is the absorption of oleic acid.

of $(\text{CdSe})_{n=1}$ and $(\text{CdSe})_{n=2}$ clusters, prepared as described in the previous section, heated at 60 °C in neat coordinating solvents (the limiting case of excess anionic surfactant): (a) oleic acid and (b) diisooctylphosphinic acid (DIOP). Heating in either oleic acid or DIOP causes a decrease in the optical density of both ($n = 1$ and $n = 2$) cluster peaks to leave spectra corresponding to metal–ligand complexes (black traces in

Figure 4a,b). This dissolution of clusters is clearly facilitated by the presence of excess ligand for Cd^{2+} , as the clusters are completely stable (no dissolution) after 60 min of heating in tetradecane, a noncoordinating solvent (Figure S3 in the SI). Consistent with a dissolution mechanism enabled by excess ligand, the cluster peaks disappear with apparent first-order kinetics, with rate constants of $3.7 \times 10^{-4} \text{ s}^{-1}$ and $3.4 \times 10^{-4} \text{ s}^{-1}$ for oleic acid and DIOP ligands, respectively (Figure 4 insets). A temperature of $60 \text{ }^\circ\text{C}$ is apparently not enough energy for dissolved monomer to add to the existing nuclei, as the cluster dissolution is not followed by any growth, and continues until the clusters are consumed.

At higher temperatures ($200 \text{ }^\circ\text{C}$, Figure 5 and $100 \text{ }^\circ\text{C}$, see SI), and in the presence of excess DIOP ligand, dissolution of

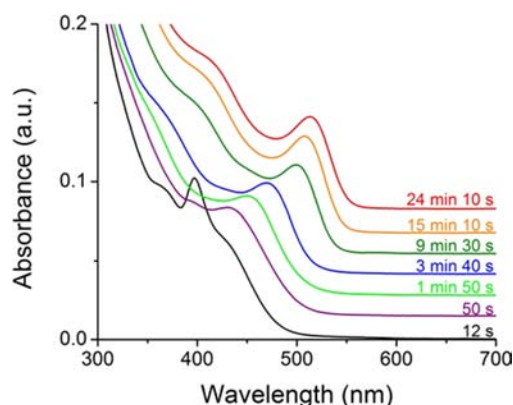


Figure 5. Temporal evolution of ground-state absorption spectra for CdSe clusters during indirect step-growth. Spectra for CdSe clusters heated at $200 \text{ }^\circ\text{C}$ with excess diisooctylphosphinic acid ligand, offset vertically for clarity. At $200 \text{ }^\circ\text{C}$ with excess ligand, clusters serve as a source of monomers for formation of a monotonically shifting distribution of QD sizes.

the $(\text{CdSe})_{n=1}$ and $(\text{CdSe})_{n=2}$ clusters into monomers is followed by addition of monomers onto existing clusters. Within this growth channel, all cluster sizes are possible, so we observe a continuously red-shifting and narrowing absorption spectrum. At $200 \text{ }^\circ\text{C}$, this progression eventually produces a distribution of CdSe quantum dots with an average diameter of $2.6 \pm 0.2 \text{ nm}$.

This process can be described as a living chain-addition polymerization, where smaller nanocrystals dissolve to create soluble monomer that adds to the larger and more stable sizes in the overall distribution. Radical chain addition involves distinct initiation, propagation, and termination steps, after which the polymer stops growing. In the growth of clusters via the mechanism we observe, the initiation step is dissolution of unstable clusters to form monomer feedstock for the propagation step ($n \rightarrow n+1$ addition), Figure 2. There is no explicit termination step in this process (similar to what was reported by Ozin and co-workers for growth of Bi_2S_3 nanowires¹⁸); rather, the size of the nanocrystals saturates when that size is large enough such that monomer feedstock is no longer produced by the initiation (dissolution) step, Figure 6a,b. Before saturation, smaller clusters (here, the $(\text{CdS})_{n=3}$ cluster at 332 nm) provide the molecular feedstock for the CdS QDs at rate ($-0.00723 \mu\text{mol/s}$) that matches the growth rate of the QDs ($0.00769 \mu\text{mol/s}$).

Figure 6c shows that the molecular weight of our CdS nanocrystal samples (as measured by the number of CdS

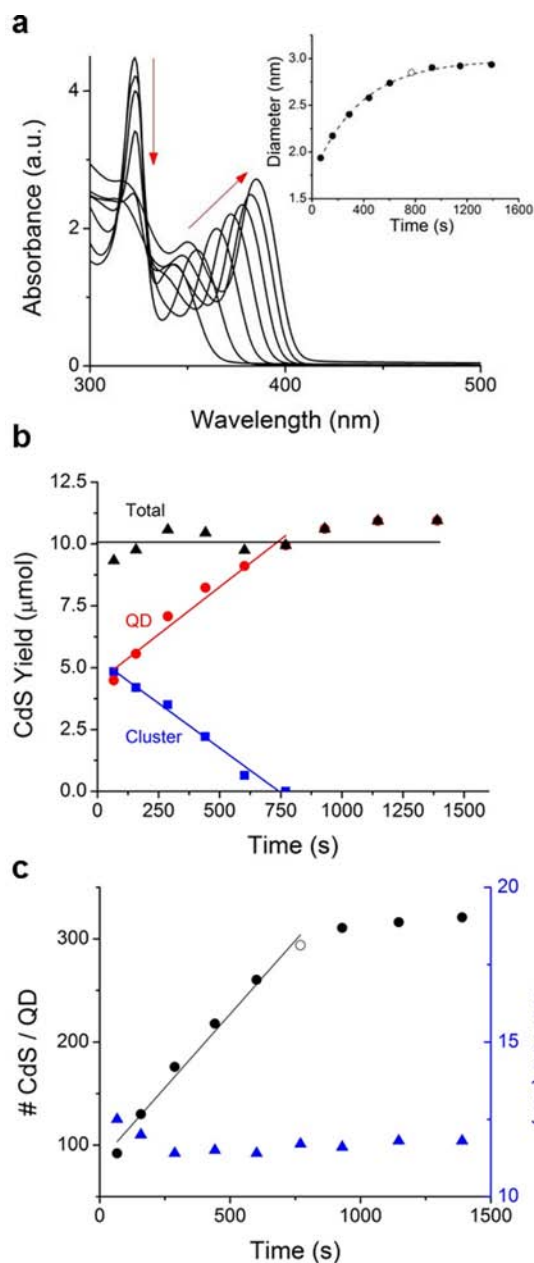


Figure 6. (a) Optical absorption spectra of CdS grown in a one-pot reaction (as opposed to heating separately prepared clusters) at $185 \text{ }^\circ\text{C}$. The increase in QD diameter reaches a maximum shortly after the disappearance of the absorption peak at 332 nm (inset, open circle), corresponding to the $(\text{CdS})_{n=3}$ cluster (b) Total of moles of CdS is conserved throughout the reaction with the magnitude of the cluster dissolution rate very similar to that of the growth rate of QDs: -0.00723 and $0.00769 \mu\text{mol/s}$, respectively. (c) Consistent with living chain-addition polymerization kinetics the QD molecular weight increases linearly, without any increase in polydispersity, until clusters react away completely (open circle).

monomer units per QD) grows linearly in time, while the size dispersity is constant with time. These two trends define a living polymerization.³⁵

The solubilization of monomer necessitates the presence of excess anionic ligand; we observe no appreciable depolymerization (only step-growth) in the absence of excess ligand. In fact, we can induce a change in mechanism from step-addition to

chain-addition by injecting DIOP into a CdSe reaction mixture that initially contained no excess ligand (see the SI, Figure S4).

Comparison of the Rates of Step-Addition and Living Chain-Addition of Clusters. A comparison of cluster growth rates for the step-growth (Figure 1b) and living chain-addition (Figure 5) mechanisms shows that larger QDs form at a faster rate by chain-addition than by step-growth at a similar temperature. On the basis of this result and our observation that larger clusters persist longer during heating than do smaller ones, we believe that a reaction between two large cluster species has a higher activation barrier than a reaction between a large cluster and a small one. A higher barrier for step-addition means that prolonged periods of heating are necessary to obtain larger sizes, and longer reaction times lead to larger polydispersity. Producing CdSe nanocrystals that absorb at visible wavelengths in the absence of excess anionic ligand necessitates high reaction temperatures (>200 °C) and, typically, several hours reaction time; therefore, results are in undesirably broad size distributions (see SI, Figure S5). High polydispersity at high molecular weight is also a distinguishing feature of organic polymers grown by step-addition. Introducing a competition between cluster dissolution and chain-addition by adding excess ligand allows us to grow larger QDs with good monodispersity (Figure 5).

The observation that $n+1$ addition occurs faster than $n + n$ addition indicates that the “equal reactivity of functional groups” concept (Flory’s assumption)—which asserts that the size of the oligomer does not dictate its reactivity during growth—does not apply for growth of clusters into QDs.²⁴ Flory’s assumption should not, in fact, apply (at least in a straightforward way) to the growth of nanocrystals because, while polymers are one-dimensional chains with a constant number of end groups, nanocrystals are three-dimensional objects, where the number of “end groups” or reactive sites available for addition depends on size (as r^2). Furthermore, the reactivity of surface sites on clusters depends on size through the surface free energy of the particle, which decreases with increasing size, and the stability of the organic passivation layer, which relies on binding affinity to the QD surface and intermolecular stabilization through van der Waals interactions. If we were able to deconvolute all of these effects from the growth kinetics, we may, in fact, find that Flory’s assumption holds for these systems, but this deconvolution would require the measurement of several ill-defined experimental parameters.

Stoichiometric Control of QD Size and Dispersity within the Living Chain-Addition Mechanism. The rules of chain-addition allow us to use chemical strategies for increasing the range of sizes we produce through this mechanism, by controlling the molar ratio anionic surfactant to Se^{2-} (or S^{2-}), the limiting ionic reagent. Panels a, b, and c of Figure 7 show absorption spectra for living chain-addition of CdS clusters with three different molar ratios of oleic acid to S^{2-} . Increasing the amount of excess surfactant increases the rate of dissolution of small clusters and therefore the rate of growth. As a result, a larger amount of smaller particles forms, and the final size of the QDs when the chain-addition reaction terminates (due to lack of monomer feedstock) decreases with increasing surfactant concentration, Figure 7d. The particles produced from this method, prior to any size-selection procedures, are as monodisperse (HWHM = 11.2–11.8 nm) as the most monodisperse CdS QDs reported in the literature for CdS QDs (HWHM = 11 nm).²⁰

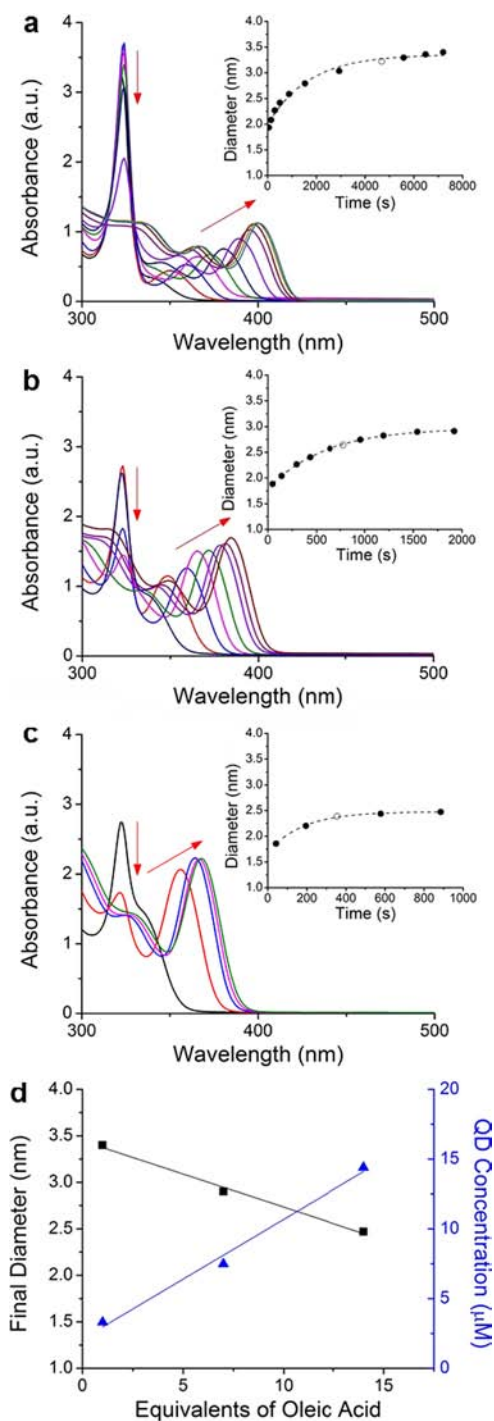


Figure 7. Optical absorption spectra for CdS produced in a one-pot reaction (as opposed to heating separately prepared clusters) at 185 °C with varying amounts of oleic acid, relative to the limiting reagent diphenylphosphine sulfide: (a) 1:1, (b) 7:1, and (c) 14:1. QD growth stops after the disappearance of clusters (insets, open circles). (d) The final diameter of QDs (squares) is inversely related to the amount of added oleic acid, while QD concentration (triangles) has the reverse trend.

CONCLUSIONS

The mechanistic parallels between the growth of QDs and the growth of polymers present an exciting opportunity to use well-established polymer science to control the molecular weight and size distributions of QDs. Here, we have taken a first step

toward this control by determining the chemical driving forces for competing step-growth and living chain-growth polymerization of cadmium chalcogenide clusters. The step-growth mechanism is operable in the growth of a number of II–VI semiconductor nanocrystals but only occurs when the reaction reaches a threshold temperature, which we believe corresponds to the activation barrier for either ligand desorption from the cluster surfaces or compression of ligand shells of the fusing clusters as they come into van der Waals contact (we are currently investigating this hypothesis). In the presence of excess anionic ligand, cluster dissolution produces a supply of molecular precursors that, at a sufficient temperature, react with clusters in solution in a living chain-growth mechanism that produces a continuous size distribution over time. Unlike step-growth, chain-growth preceded by dissolution allows for larger QDs to grow without extended periods of high-temperature heating that causes polydispersity.

The fact that the two chemical routes for growth of QDs mirror growth mechanisms typically observed in organic polymerizations is not surprising, considering that QDs possess the intrinsic unit cell of the bulk semiconductor lattice, which is analogous to an inorganic polymer backbone. In addition to the nanocrystal literature we cited in the Discussion, the step-growth mechanism has been observed for molecular systems such as cadmium phosphorodiselenoate complexes,³⁶ monomeric arsenogallane,³⁷ and ligated Pd₂Te₂ rhombohedral units³⁸ which all undergo dimerization to eventually form larger cluster species and polymers.

We propose that the step-growth-type fusion between clusters of specific nuclearity in the absence of excess ligand is responsible not only for the quantized growth apparent in the absorption spectra of these reaction mixtures but also for the consistent observation of certain sizes of clusters. Rather than being the consequence of thermodynamically stable closed-shell geometries, so-called “magic-sized” clusters are sizes that are integer multiples of some base unit that undergoes fast nucleation. Our observation of a continuous distribution of cluster sizes during polymerization in the presence of excess ligand further disputes the theory of a set of particularly thermodynamically stable cluster sizes.

■ ASSOCIATED CONTENT

Supporting Information

Full experimental procedures and additional cluster growth kinetics. This material is available free of charge via the Internet at <http://pubs.acs.org>.

■ AUTHOR INFORMATION

Corresponding Author

e-weiss@northwestern.edu

Notes

The authors declare no competing financial interest.

■ ACKNOWLEDGMENTS

This work was supported by the Army Research Office through a Presidential Early Career Award for Scientists and Engineers (PECASE) to E.A.W.

■ REFERENCES

- (1) Fojtik, A.; Weller, H.; Koch, U.; Henglein, A. *Ber. Bunsen. Phys. Chem.* **1984**, *88*, 969–977.
- (2) Peng, Z. A.; Peng, X. *J. Am. Chem. Soc.* **2002**, *124*, 3343–3353.

- (3) Herron, N.; Calabrese, J. C.; Farneth, W. E.; Wang, Y. *Science* **1993**, *259*, 1426–1428.
- (4) Vossmeier, T.; Reck, G.; Katsikas, L.; Haupt, E. T. K.; Schulz, B.; Weller, H. *Science* **1995**, *267*, 1476–1479.
- (5) Soloviev, V. N.; Eichhofer, A.; Fenske, D.; Banin, U. *J. Am. Chem. Soc.* **2000**, *122*, 2673–2674.
- (6) Kudera, S.; Zanella, M.; Giannini, C.; Rizzo, A.; Li, Y.; Gigli, G.; Cingolani, R.; Ciccarella, G.; Spahl, W.; Parak, W. J.; Manna, L. *Adv. Mater.* **2007**, *19*, 548–552.
- (7) Bowers, M. J., II; McBride, J. R.; Rosenthal, S. J. *J. Am. Chem. Soc.* **2005**, *127*, 15378–15379.
- (8) Evans, C. M.; Guo, L.; Peterson, J. J.; Maccagnano-Zacher, S.; Krauss, T. D. *Nano Lett.* **2008**, *8*, 2896–2899.
- (9) Wang, Y.; Liu, Y.-H.; Zhang, Y.; Wang, F.; Kowalski, P. J.; Rohrs, H. W.; Loomis, R. A.; Gross, M. L.; Buhro, W. E. *Angew. Chem., Int. Ed.* **2012**, *51*, 6154–6157.
- (10) Kasuya, A.; Sivamohan, R.; Barnakov, Y. A.; Dmitruk, I. M.; Nirasawa, T.; Romanyuk, V. R.; Kumar, V.; Mamykin, S. V.; Tohji, K.; Jayadevan, B.; Shinoda, K.; Kudo, T.; Terasaki, O.; Liu, Z.; Belosludov, R. V.; Sundararajan, V.; Kawazoe, Y. *Nat. Mater.* **2004**, *3*, 99–102.
- (11) Sanville, E.; Burnin, A.; BelBruno, J. J. *J. Phys. Chem. A* **2006**, *110*, 2378–2386.
- (12) Nguyen, K. T.; Day, P. N.; Pachter, R. *J. Phys. Chem. C* **2010**, *114*, 16197–16209.
- (13) Colvin, V. L.; Schlamp, M. C.; Alivisatos, A. P. *Nature* **1996**, *37*, 354–357.
- (14) Medintz, I. L.; Uyeda, H. T.; Goldman, E. R.; Mattoussi, H. *Nat. Mater.* **2005**, *4*, 435–446.
- (15) Alivisatos, P. *Nat. Biotechnol.* **2004**, *22*, 47–52.
- (16) Jiang, Z.-J.; Kelley, D. F. *ACS Nano* **2010**, *4*, 1561–1572.
- (17) Cossairt, B. M.; Owen, J. S. *Chem. Mater.* **2011**, *23*, 3114–3119.
- (18) Cademartiri, L.; Guerin, G.; Bishop, K. J. M.; Winnik, M. A.; Ozin, G. A. *J. Am. Chem. Soc.* **2012**, *134*, 9327–9334.
- (19) Evans, C. M.; Evans, M. E.; Krauss, T. D. *J. Am. Chem. Soc.* **2010**, *132*, 10973–10975.
- (20) Yu, W. W.; Qu, L.; Guo, W.; Peng, X. *Chem. Mater.* **2003**, *15*, 2854–2860.
- (21) Boldt, K.; Bruns, O. T.; Gaponik, N.; Eychmuller, A. *J. Phys. Chem. B* **2006**, *110*, 1959–1963.
- (22) Aldana, J.; Wang, Y. A.; Peng, X. *J. Am. Chem. Soc.* **2001**, *123*, 8844–8850.
- (23) Gomes, R. H., A.; Szczygiel, A.; Zhao, Q.; Vantomme, A.; Martins, J. C.; Hens, Z. *J. Am. Chem. Soc.* **2010**, *132*, 10195–10201.
- (24) Odian, G. *Principles of Polymerization*, 4th ed.; John Wiley and Sons: Hoboken, NJ, 2004.
- (25) Dukes, I., A.D.; McBride, J. R.; Rosenthal, S. J. *Chem. Mater.* **2010**, *22*, 6402–6408.
- (26) Liu, Y.-H.; Wang, F.; Wang, Y. A.; Gibbons, P. C.; Buhro, W. E. *J. Am. Chem. Soc.* **2011**, *133*, 17005–17013.
- (27) Zanella, M.; Abbasi, A. Z.; Schaper, A. K.; Parak, W. J. *J. Phys. Chem. C* **2010**, *114*, 6205–6215.
- (28) Li, M.; Ouyang, J.; Ratcliffe, C. I.; Pietri, L.; Wu, X.; Leek, D. M.; Moudrakovski, I.; Lin, Q.; Yang, B.; Yu, K. *ACS Nano* **2009**, *3*, 3832–3838.
- (29) Liu, K.; Nie, Z.; Zhao, N.; Li, W.; Rubinstein, M.; Kumacheva, E. *Science* **2010**, *329*, 197–200.
- (30) Ribiero, C.; Lee, E. J. H.; Longo, E.; Leite, E. R. *ChemPhysChem* **2006**, *7*, 664–670.
- (31) Newton, J. C.; Ramasamy, K.; Mandal, M.; Joshi, G. K.; Kumbhar, A.; Sardar, R. *J. Phys. Chem. C* **2012**, *116*, 4380–4389.
- (32) Sun, M.; Yang, X. *J. Phys. Chem. C* **2009**, *113*, 8701–8709.
- (33) Shanbhag, S.; Tang, Z.; Kotov, N. A. *ACS Nano* **2007**, *1*, 126–132.
- (34) Colfen, H.; Mann, S. *Angew. Chem.* **2003**, *42*, 2350–2365.
- (35) Matyjaszewski, K. P.; Patten, T.E.; Xia, J. *J. Am. Chem. Soc.* **1997**, *119*, 674.
- (36) Liu, C. W.; Lobana, T. S.; Santra, B. K.; Hung, C.-M.; Liu, H.-Y.; Liaw, B.-J.; Wang, J.-C. *Dalton Trans.* **2006**, 560–570.

(37) Byrne, E. K.; Parkanyi, L.; Theopold, K. H. *Science* **1988**, *241*, 332–334.

(38) Brennan, J. G.; Siegrist, T.; Stuczynski, S. M.; Steigerwald, M. L. *J. Am. Chem. Soc.* **1990**, *112*, 9233–9236.